The Clay Minerals Society Workshop Lectures Series, Vol. 21 (2016), Chapter 20, 251–257

DIFFUSION MODEL CONSIDERING MULTIPLE PORE STRUCTURES IN COMPACTED BENTONITE

KENJI YOTSUJI[1]*, YUKIO TACHI[1], and TAKAHIRO OHKUBO[2]

[1]*Japan Atomic Energy Agency, 4-33, Muramatsu, Tokai-mura, Ibaraki, 319-1194, Japan*
[2]*Chiba University, 1-33, Yayoi-cho, Inage-ku, Chiba, 263-8522 Japan*
**e-mail: yotsuji.kenji@jaea.go.jp*

Sorption and diffusion of radionuclides in compacted clays and argillaceous rocks are key processes in the safe geological disposal of radioactive waste. The integrated sorption and diffusion (ISD) model was developed to quantify radionuclide transport in compacted bentonite. The current ISD model is based on a simplified pore structure with averaged pore aperture and the Gouy-Chapman electric double layer (EDL) theory and can account quantitatively for the diffusion of monovalent cations and anions under different conditions (*e.g.* porewater salinity and bentonite density). In the present study a modified ISD model was developed which considers multiple pore structures, including interlayer and interparticle pores, particularly for anionic species, in order to improve the applicability of the existing model. The applicability of the modified ISD model to multiple pore structures was tested. The dual-pore model, which considers only interparticle pores and averaged interlayer pores, performed adequately as an heterogeneous pore model.

1. Introduction

Diffusion and sorption of radionuclides in compacted bentonite are key processes in the safe geological disposal of radioactive waste. The ISD model (Ochs *et al.*, 2001; Tachi *et al.*, 2010; Tachi and Yotsuji, 2012, 2014) considers porewater chemistry, sorption, and diffusion in compacted bentonite. In the ISD model, the diffusion component based on the EDL theory accounts consistently for excess cation diffusion and anion exclusion in narrow pores. The current ISD model (Tachi and Yotsuji, 2014) can account quantitatively for diffusion data of monovalent cations and anions; the model predictions disagree, however, with the diffusion data of multivalent-cation and complex species (Tachi *et al.*, 2010; Tachi and Yotsuji, 2012). The current ISD model assumes the classical Gouy-Chapman (G-C) model of the EDL theory and the homogeneous pore model. To improve the applicability of the model, evaluation of the effects of more realistic diffusion models by considering atomic-level interactions among solute, solvent, or clay mineral and the heterogeneous pore structure is important. To this end, as a first step, modified models which consider the excluded volume effect and the dielectric saturation effect were tested (Yotsuji *et al.*, 2014), although these modified models had little effect on effective diffusivity. In contrast, the model which

DOI: 10.1346/CMS-WLS-21.20

considers the effective electric charge of hydrated ions, calculated using the Gibbs free energy of hydration, agreed well with the diffusion data on divalent cations (Sr^{2+}). As a next step, in the present study, the existing ISD model was modified to allow for consideration of multiple pore structures, including interlayer and interparticle pores. The applicability of the modified ISD model was then tested for multiple pore structures.

2. Modeling approach

The key parameter of the diffusion component $D_{e,i}$ ($m^2\ s^{-1}$) of species i in the ISD model is electrostatic constrictivity $\delta_{el,i}$ (-), and these are related as follows:

$$D_{e,i} = \phi \frac{\delta_g \delta_{el,i}}{\tau^2} D_{w,i}, \tag{1}$$

where ϕ is porosity (-), τ is tortuosity (-), δ_g is the geometrical constrictivity (-), and $D_{w,i}$ is the tracer diffusivity of species i in bulk liquid water ($m^2\ s^{-1}$). The electrostatic constrictivity is evaluated as the average ratio of the ionic concentration in the diffuse layer *vs.* that in bulk water, by considering the enhanced viscosity of water due to viscoelectric effects in the interlayer as follows:

$$\begin{aligned}\delta_{el,i}: &= \frac{1}{d}\int_0^d \frac{\eta_0}{\eta(x)} \cdot \frac{n_i(x)}{n_{b,i}}\, dx \\ &= \frac{1}{d}\int_0^d \frac{1}{1 + f_{ve}(d\psi/dx)^2} \exp\left(-\frac{ez_i\psi(x)}{kT}\right) dx\end{aligned} \tag{2}$$

where $n_i(x)$, $\eta(x)$, and $\psi(x)$ are the local number density of ionic species i (m^{-3}), viscosity of water (N s m^{-2}), and electric potential (V) in the interlayer at a distance of x (m) from the clay basal surface, respectively; $n_{b,i}$ and η_0 are the corresponding number density and the viscosity of bulk water, respectively; d is the interlayer width (m); z_i is the valence of ionic species i (-); e is the absolute value of the elementary electric charge (C); k is Boltzmann's constant (J K^{-1}); T is the temperature (K); and f_{ve} is a viscoelectric constant ($=1.02 \times 10^{-15}$ $m^2\ V^{-2}$, Lyklema and Overbeek, 1961).

The Poisson-Boltzmann (P-B) equation, which describes the distribution of electric potential $\psi(x)$ in the EDL, is as follows (*e.g.* Verwey and Overbeek, 1948):

$$\frac{d^2\psi}{dx^2} = -\frac{1}{\varepsilon_b \varepsilon_0} \sum_i ez_i n_{b,i} \exp\left(-\frac{ez_i\psi(x)}{kT}\right),$$

$$\left.\frac{d\psi}{dx}\right|_{x=0} = -\frac{\sigma_0}{\varepsilon_b \varepsilon_0},\ \left.\frac{d\psi}{dx}\right|_{x=d/2} = 0$$

where ε_b is the relative permittivity of water (= 78.36 at 298.15 K) and ε_0 is the vacuum permittivity (C V^{-1} m^{-1}). Surface charge density, σ_0, is -0.129 C m^{-2}, as calculated from the CEC (= 108 meq/100 g) and specific surface area (= 8.1×10^5 m^2 kg^{-1}) for montmorillonite (Carter *et al.*, 1965). The entire pore volume is assumed to be distributed in slit-like pores with an averaged aperture of $d = 2.25 \times 10^{-9}$ m, as calculated for Kunipia-F® (purified montmorillonite, which is produced from a crude Tsukinuno bentonite) at a dry density of 800 kg m^{-3}. $D_{e,i}$ values were evaluated based on equation 1 using the same porosity ϕ (= 0.723) and geometric factor δ_g/τ^2 (= 0.0989, Tachi and Yotsuji, 2014) for both cations and anions.

As mentioned above, the existing ISD model was developed on the assumption of an homogeneous pore structure. According to analyses using X-ray diffraction (XRD) or nuclear magnetic resonance (NMR), however, the migration pathways of nuclides as (1) 'interlayer (interlamellar) pores' (in montmorillonite) and (2) 'interparticle pores' (between clay particles or other mineral particles) in saturated compacted bentonite (*e.g.* Bradbury and Bayens, 2003) must be classified. This pore structure changes according to the dry density of bentonite and the salinity of porewater (Kozaki *et al.*, 1998, 2008; Holmboe *et al.*, 2012).

The simplest modification of the ISD model is that which accounts for heterogeneous pore structures; the dual-pore model is considered first (Figure 1a). Here, T_1 is the thickness of a montmorillonite 2:1 layer (m), b is the basal spacing (a period of the direction perpendicular to a basal plane) (m), T_2 is averaged thickness of accessory minerals included in the dual pore structure unit cell (m), d_1 (= $b - T_1$) is interlayer spacing (m), and d_2 is averaged spacing of interparticle pores (m). S is the area of one side of the basal plane (m^2) and it satisfies $S = S_w M_m/(2N)$, where S_w is the specific surface area of montmorillonite (m^2 kg^{-1}), M_m is the molecular weight of the montmorillonite included in a unit cell (kg), and N is the stacking number of the montmorillonite 2:1 layer included in a unit cell. Interlayer spacing, d_1, is calculated on the basis of the relationship $T_1 = 2/(S_w\ \rho_m)$ as follows:

$$d_1 = b - \frac{2}{S_w \rho_m} \tag{4}$$

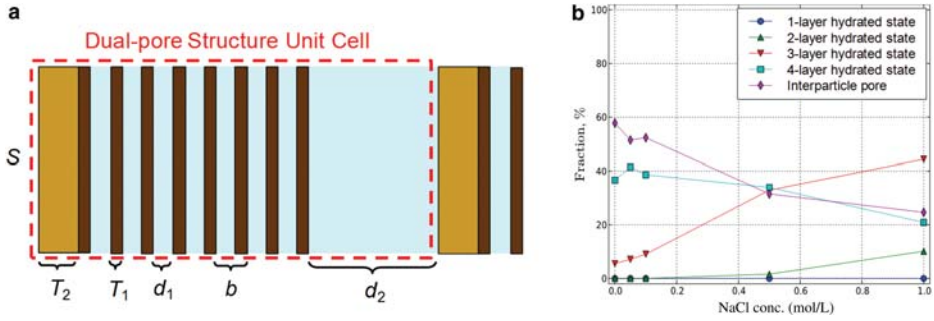

Figure 1. (a) Schematic diagram of the unit cell of a dual-pore model, and (b) salinity dependence of the volume ratio of a one-to-four-layer hydrated state and interparticle pores with ρ_b^{ben} = 800 kg m^{-3} (JAEA, 2015).

where ρ_m (= 2884 kg m^{-3}) is the specific density of pure montmorillonite. Then, the average spacing of interparticle pores, d_2, is calculated using the following equation:

$$d_2 = \frac{2N}{S_w r}\left(\frac{1}{\rho_b^{ben}} - \frac{1}{\rho_s^{ben}}\right) - (N-1)d_1 \quad (5)$$

where ρ_s^{ben} and ρ_b^{ben} are the specific and dry densities of bentonite, respectively, and r is the montmorillonite content in bentonite. When the dual-pore model is applied to Kunipia-F ($\rho_s^{ben} = 2880$ kg m^{-3}, $r = 0.99$) with $\rho_b^{ben} = 800$ kg m^{-3}, the montmorillonite interlayers are mostly in the three-layer hydrated state, and the basal spacing $b = 1.88 \times 10^{-9}$ m (Kozaki *et al.*, 1998). In the present study, $S_w = 8.1 \times 10^5$ m^2 kg^{-1} was used. $T_1 = 8.56 \times 10^{-10}$ m and interlayer spacing, $d_1 = 1.02 \times 10^{-9}$ m, therefore. Furthermore, assuming that averaged stacking number N is equal to 8 (Nakano, 1991), the average spacing of interparticle pores, d_2 is equal to 1.09×10^{-8} m, according to equation 5.

In the development of the dual-pore model, the salinity dependence of the interlayer hydrated state was ignored. The interlayer hydrated state depends mostly on salinity, and various hydration states coexist. Using the result of an NMR measurement based on the method described by Ohkubo *et al.* (2008), a multi-pore model is considered here which takes into account the salinity dependence of the interlayer hydrated state and the coexistence of various hydration states (JAEA, 2015). The salinity dependence of the volume ratios of one-to-four-layer hydrated states and interparticle pores with $\rho_b^{ben} = 800$ kg m^{-3} is shown in Figure 1b. The averaged spacing of interparticle pores, d_2, is calculated using the following equation:

$$d_2 = \frac{1 - f_{\varepsilon 1}}{f_{\varepsilon 1}}(N-1)d_1 \quad (6)$$

where $f_{\varepsilon 1}$ is the volume ratio of montmorillonite interlayer pores to the total pore volume in bentonite, and interlayer spacing, d_1, is defined by the following equation:

$$d_1 = \left(\frac{\xi_1}{d_{1-1}} + \frac{\xi_2}{d_{1-2}} + \frac{\xi_3}{d_{1-3}} + \frac{1 - \xi_1 - \xi_2 - \xi_3}{d_{1-4}}\right)^{-1} \quad (7)$$

where ξ_i is the volume ratio of the ith layer hydrated interlayer pores to the total interlayer pore volume, and $d_{1\text{-}i}$ is the ith layer hydrated interlayer spacing. According to XRD measurements (Kozaki *et al.*, 1998), the basal spacing of the two-layer hydrated state, b, was 1.56×10^{-9} m, and the basal spacing of the three-layer hydrated state, b, was 1.88×10^{-9} m. The two-layer hydrated interlayer spacing, d_{1-2}, therefore equals 7.04×10^{-10} m, and the three-layer hydrated interlayer spacing, d_{1-3}, equals 1.02×10^{-9} m where $T_1 = 8.56 \times 10^{-10}$ m. The one-layer hydrated interlayer spacing, d_{1-1}, and four-layer hydrated interlayer spacing, d_{1-4}, were estimated from these data assuming a linear relationship between hydrated state and interlayer spacing. As a result, $d_{1-1} = 3.84 \times 10^{-10}$ m and $d_{1-4} = 1.34 \times 10^{-9}$ m.

3. Results and discussion

The salinity dependence of the effective diffusivity of $Sr^{2+}/Cs^{+}/I^{-}$ calculated using the dual-pore model and the current ISD model are shown in Figure 2a, together with measured data (Tachi and Yotsuji, 2012, 2014). The effective diffusivities were calculated using harmonic mean weighting in conjunction with the volume ratio of the logarithmic effective diffusivity of each pore. The cationic species migrate mainly in the narrower interlayer pores because of enhanced cation concentration. In contrast, anionic species are expected to migrate into wider pores forced by anion exclusion in narrow pores (Tachi and Yotsuji, 2014). The dependence of salinity of electrostatic constrictivity on wider pore spacing is less than that on narrower pore spacing. Anionic species have this tendency in contrast to cationic species. The dependence of effective diffusivity on the salinity in the dual-pore model is, therefore, less than that in the homogeneous pore model (current ISD model) because the contribution of interparticle pores to effective diffusivity is greater than that of interlayer pores. This situation is almost the same in the case of the multi-pore model (Figure 2b) where it is more conspicuous than for the dual-pore model because the volume ratio of pores with wider spacing is greater in lower-salinity domains (Figure 1b).

In the present study, the specific surface area of montmorillonite (S_w) was assumed to be $8.1 \times 10^5\ m^2\ kg^{-1}$ (Carter *et al.*, 1965) and the specific density of pure montmorillonite (ρ_m) to be $2884\ kg\ m^{-3}$ (calculated on the basis of $\rho_s^{ben} = 2880\ kg\ m^{-3}$ and $r = 0.99$ for Kunipia-F). Then, $T_1 = 8.56 \times 10^{-10}$ m, calculated from the relationship $T_1 = 2/(S_w \rho_m)$, was used. According to recent literature (*e.g.* Karnland *et al.*, 2006; Holmboe *et al.*, 2012; Holmboe and Bourg, 2014), however, for $S_w = 7.5 \times 10^5\ m^2\ kg^{-1}$ and $\rho_m = 2800\ kg\ m^{-3}$, T_1 is evaluated as 9.5×10^{-10} m, therefore. Although the difference of 1×10^{-10} m in the thickness of the clay is non-negligible, confirmation was achieved here that it would have little influence on the final results of the diffusion models.

The current ISD model could be improved by considering multiple pore structures, particularly for anionic species, and the dual-pore model, which considers only interparticle

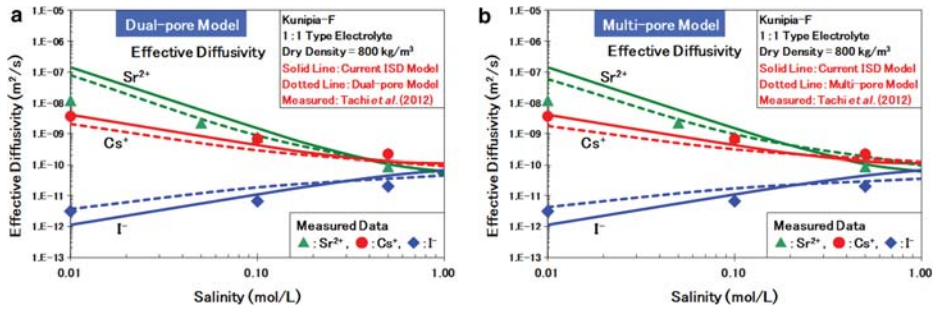

Figure 2. (a) Effective diffusivity of $Sr^{2+}/Cs^{+}/I^{-}$ as a function of salinity, as calculated using the dual-pore model and the current ISD model (homogeneous pore model), together with measured data (Tachi and Yotsuji, 2012, 2014); (b) the same result determined using a multi-pore model.

pores and averaged interlayer pores, performed as an heterogeneous pore model. The effective diffusivity of ionic species was influenced heavily by porewater salinity, but almost never depended on the geometrical microstructures of compacted bentonite pores under the fixed dry density of bentonite because the electrical effects at the microscale (*e.g.* EDL) persist up to the macroscale diffusion parameter, but the geometrical microstructures (*e.g.* tortuosity and pore volume ratio) are homogenized upon scaling up.

Acknowledgments

This study was conducted partly as 'The project for validating assessment methodology in a geological disposal system' funded by the Ministry of Economy, Trade and Industry of Japan.

Guest editor: Reiner Dohrmann

The authors and editors are grateful to anonymous reviewers who offered very helpful input and suggestions. A list of all reviewers is given at the end of the Preface for this volume.

References

Bradbury, M.H. and Baeyens, B. (2003) Porewater chemistry in compacted re-saturated MX-80 bentonite. *Journal of Contaminant Hydrology*, **61**, 329–338.

Carter, D.L., Heilman, M.D., and Gonzalez, C.L. (1965) Ethylene glycol monoethyl ether for determining surface area of silicate minerals. *Soil Science*, **100**, 356–360.

Holmboe, M. and Bourg, I.C. (2014) Molecular dynamics simulations of water and sodium diffusion in smectite interlayer nanopores as a function of pore size and temperature. *Journal of Physical Chemistry C*, **118**, 1001–1013.

Holmboe, M., Wold, S., and Jonsson, M. (2012) Porosity investigation of compacted bentonite using XRD profile modeling. *Journal of Contaminant Hydrology*, **128**, 19–32.

Japan Atomic Energy Agency (JAEA) (2015) The project for validating assessment methodology in geological disposal system. *H26 report of Japanese project entrusted by the Ministry of Economy, Trade and Industry (METI) of Japan*.

Karnland, O., Olsson, S., and Nilsson, U. (2006) Mineralogy and sealing properties of various bentonites and smectite-rich clay material. *Swedish Nuclear Fuel and Waste Management Co.*, SKB TR-06-30.

Kozaki, T., Fujishima, A., Sato, S., and Ohashi, H. (1998) Self-diffusion of sodium ions in compacted montmorillonite. *Nuclear Technology*, **121**, 63–69.

Kozaki, T., Liu, J., and Sato, S. (2008) Diffusion mechanism of sodium ions in compacted montmorillonite under different NaCl concentration. *Physics and Chemistry of the Earth*, **33**, 957–961.

Lyklema, J. and Overbeek, J.Th.G. (1961) On the interpretation of electrokinetic potentials. *Journal of Colloid Science*, **16**, 501–512.

Nakano, M. (1991) *Mass Transfer within Soils.* University of Tokyo Press, Tokyo, 187 pp. (in Japanese).

Ochs, M., Lothenbach, B., Wanner, H., Sato, H., and Yui, M. (2001) An integrated sorption/diffusion model for the calculation of consistent distribution and diffusion coefficients in compacted bentonite. *Journal of Contaminant Hydrology*, **47**, 283–296.

Ohkubo, T., Kikuchi, H., and Yamaguchi, M. (2008) An approach of NMR relaxometry for understanding water in saturated compacted bentonite. *Physics and Chemistry of the Earth*, **33**, S169–S176.

Tachi, Y. and Yotsuji, K. (2012) Diffusion and sorption of Sr^{2+} in compacted sodium montmorillonite as a function of porewater salinity. In: Abstract Volume of the 5th international meeting: "Clays in Natural and Engineered Barriers for Radioactive Waste Confinement", Montpellier, France.

Tachi, Y. and Yotsuji, K. (2014) Diffusion and sorption of Cs^{+}, Na^{+}, I^{-} and HTO in compacted sodium montmorillonite as a function of porewater salinity: Integrated sorption and diffusion model. *Geochimica et Cosmochimica Acta*, **132**, 75–93.

Tachi, Y., Nakazawa, T., Ochs, M., Yotsuji, K., Suyama, T., Seida, Y., Yamada, N., and Yui, M. (2010) Diffusion and sorption of neptunium(V) in compacted montmorillonite: effects of carbonate and salinity. *Radiochimica Acta*, **98**, 711–718.

Verwey, E.J.W. and Overbeek, J.Th.G. (1948) *Theory of the Stability of Lyophobic Colloids.* Elsevier, Amsterdam, 218 pp.

Yotsuji, K., Tachi, Y., and Nishimaki, Y. (2014) Diffusion modeling in compacted bentonite based on modified Gouy-Chapman model. *Materials Research Society Symposium Proceedings*, **1665**, 123–129.